Mixed quantum-classical molecular dynamics: Aspects of the multithreads algorithm

Chun-Cheng Wan and Jeremy Schofield
Chemical Physics Theory Group, Department of Chemistry, University of Toronto, Toronto, Ontario, Canada M5S 3H6

(Received 1 June 2000; accepted 7 August 2000)

The mixed quantum-classical Liouville equation is derived from a semiclassical perspective starting from the full quantum Schrödinger equation. An asymptotic numerical scheme for solving the equation is discussed which relies on propagating swarms of interacting ''threads'' which represent the density matrix or other observable. It is demonstrated that this ''multithreads'' method performs extremely well on simple one-dimensional model systems designed to test nonadiabatic molecular dynamic methods, yielding essentially exact results for a variety of models. © *2000 American Institute of Physics.* [S0021-9606(00)71441-3]

I. INTRODUCTION

Great effort has been made in recent years to develop procedures that incorporate quantum transitions into a classical evolution scheme.[1–13] The goal of mixed quantum-classical dynamical methods is to provide a simplified description of the dynamics of large systems in which quantum mechanical behavior such as tunneling, interference and level quantization is significant. For some systems, full quantum calculations such as the full multiple spawning (FMS) method are possible when quantum effects are spatially and temporally localized.[12] Although these methods are promising, it is appealing to simplify the level of description to describe the heavy particle motions in a classical framework, particularly for very large systems of biological importance.

One approach to incorporating quantum effects into a classical framework is based upon semiclassical methods,[14] such as the initial-value representation (IVR),[15] and its simplified versions (LSC-IVR).[16] Although semiclassical methods are attractive because they treat classical and quantum degrees of freedom on equal footing, accurate calculations using IVR methods tend to be computationally intensive due to slow convergence of oscillatory integrands. Furthermore, the approximations made to obtain tractable expressions for transition probabilities and time-correlation functions are fairly subtle and difficult to control. In addition, most semiclassical methods do not take advantage of the fact that the quantum interactions typically involve relatively few energy surfaces, and perhaps involve an unnecessary amount of computation.

In contrast, the mixed quantum-classical molecular approach to nonadiabatic systems separates the full system into ''classical'' and quantum subsystems which interact with one another dynamically. This separation into quantum and classical components allows important simplifications through simple approximations which are valid in particular representations of the quantum subsystem. The mixed quantum-classical formalism is usually based on either ad-hoc rules for the mixed quantum-classical system evolution,[2,3] or on stationary-phase approximations of reduced path integral propagators.[5–7,17] In practice, mixed quantum-classical methods are often implemented through a stochastic ''surface-hopping'' algorithm[18] in which the classical evolution occurs with Hellmann–Feynman forces on a single, statistically chosen adiabatic energy surface. However, as the surface-hopping rules are usually somewhat arbitrary in nature, it is difficult to define a correct set of transition rules relevant over all energy ranges.

Another promising avenue for incorporating quantum effects into classical molecular dynamics is based on the mixed quantum-classical Liouville equation.[9,10,19,20] This evolution equation can be obtained utilizing a systematic expansion in the ratio of the masses of the quantum and classical degrees of freedom of the exact evolution equation for the partial Wigner transformation of the density matrix.[10] In a recent article,[21] an asymptotic method of solving the mixed quantum-classical Liouville equation, termed the *multithreads method*, was proposed. The multithreads method relies on a finite representation of the partially Wigner transformed density matrix in which a set of grid points or ''threads'' for each of the matrix elements of the density matrix evolves exactly. In this approach, the nonadiabatic transitions correspond to quantum rotations of the matrix elements and branching of the thread trajectories. The method was demonstrated to give essentially exact quantitative results for a simple proton transfer model. A similar method[9] has appeared in the literature which utilizes a different grid propagation scheme and an extrapolation method to estimate the density matrix at each time step.

In this article, we first demonstrate that an equivalent quantum-classical Liouville equation can be derived by approximating the nuclear part of the full wave function with a semiclassical wave function. In Sec. III, the multithreads solution method is examined in detail, and its performance is evaluated on standard models[3] developed specifically to test nonadiabatic molecular dynamics methods. The numerical simulations are compared to solutions obtained from the exact quantum evolution of the system as well as those obtained from other approximate methods. From the numerical studies, it is evident that the multithreads solutions converge

rapidly to the exact results for a small number of total threads for all models considered. Finally, in Sec. IV we discuss briefly extensions of the solution method to large systems and compare the multi-threads algorithm to other propagation schemes.

II. THE MIXED QUANTUM AND CLASSICAL DENSITY MATRIX AND THE SEMICLASSICAL APPROXIMATION

A. The quantum-classical Liouville equation

The correct form of the mixed quantum-classical Liouville equation was suggested by Boucher and Traschen[19] by examining the simplest evolution equation for a mixed quantum-classical system consistent with a set of natural requirements for a semiclassical theory which extends both quantum and classical systems. It has subsequently been derived in a systematic fashion using both algebraic structures[20,22] and Wigner transform methods.[9,10] For the sake of completeness, we outline how the quantum-classical Liouville equation can be obtained by partial Wigner transform techniques.

Consider a general quantum system consisting of n quantum particles of mass m and N particles of mass M with a Hamiltonian of the form,

$$\hat{H}=\frac{\hat{P}^2}{2M}+\frac{\hat{p}^2}{2m}+\hat{V}(\hat{q},\hat{Q}), \tag{1}$$

where $\hat{P}$, $\hat{p}$, $\hat{Q}$, and $\hat{q}$ are vectors of momentum and position operators of the classical and quantum degrees of freedom. The total potential energy $\hat{V}$ may be written as $\hat{V}_q(\hat{q})+\hat{V}_{\rm cl}(\hat{Q})+\hat{V}_{\rm co}(\hat{Q},\hat{q})$, where the subscripts refer to the quantum, classical and coupling terms in the potential energy. The evolution of any dynamical observable $\hat{B}$ is given by the Heisenberg equation,

$$\frac{d\hat{B}}{dt}=\frac{i}{\hbar}[\hat{H},\hat{B}]. \tag{2}$$

In order to focus on the limit in which the particles with mass M, with $M\gg m$, are treated classically, it is convenient to perform a partial Wigner transform of Eq. (2) with respect to the classical degrees of freedom $\hat{Q}$ defined as

$$\hat{B}_w(R,P)=\frac{1}{(2\pi\hbar)^{3N/2}}\int dz e^{iP\cdot z/\hbar}\left\langle R-\frac{z}{2}\middle|\hat{B}\middle|R+\frac{z}{2}\right\rangle, \tag{3}$$

where R is the coordinate representation of the operator $\hat{Q}$. Note that $\hat{B}_w(R,P)$ is still an operator in the quantum subspace. In the limit in which the masses of the bath (classical) particles are much larger than the quantum particle masses, a small parameter $\eta=(m/M)^{1/2}$ may be defined and used to perturbatively order terms[10] in the equations of motion for a partially Wigner transformed dynamical observable $\hat{B}_w(R,P)$. If terms up to first order in ϵ are retained in the full equation of motion, a Liouville equation for the mixed quantum-classical system is obtained,[10]

$$\begin{aligned}\frac{d\hat{B}_w(R,P,t)}{dt}&=\frac{i}{\hbar}[\hat{H}_w(R,P),\hat{B}(R,P,t)]\\&\quad-\tfrac{1}{2}(\{\hat{H}_w(R,P),\hat{B}_w(R,P,t)\}\\&\quad-\{\hat{B}_w(R,P,t),\hat{H}_w(R,P)\})\\&=i\mathcal{L}\hat{B}_w(R,P,t),\end{aligned} \tag{4}$$

where the Poisson bracket notation in Eq. (4) signifies

$$\begin{aligned}\{\hat{H}_w(R,P),\hat{B}_w(R,P)\}&=\nabla_R\hat{H}_w(R,P)\cdot\nabla_P\hat{B}_w(R,P)\\&\quad-\nabla_P\hat{H}_w(R,P)\cdot\nabla_R\hat{B}_w(R,P),\end{aligned} \tag{5}$$

and the partial Wigner transform of the Hamiltonian is

$$\hat{H}_w(R,P)=\frac{P^2}{2M}+\frac{\hat{p}^2}{2m}+\hat{V}_w(R,\hat{q})=\frac{P^2}{2M}+\hat{h}_w(R,P). \tag{6}$$

It is important to note that in Eq. (4), total energy is conserved *by construction* regardless of the choice of quantum subsystem representation. Similarly, the evolution equation for the partial Wigner transform $\hat{\rho}_w$ of the full density matrix $\hat{\rho}$ (henceforth abbreviated PWTDM) can be written as

$$\frac{\partial\hat{\rho}_w(R,P,t)}{\partial t}=-i\mathcal{L}\hat{\rho}_w(R,P,t). \tag{7}$$

The mixed quantum-classical Liouville equation can be represented in an arbitrary time-independent basis which depends parametrically on the classical coordinates R as

$$\begin{aligned}\frac{\partial\hat{\rho}_w^{\alpha\beta}(R,P,t)}{\partial t}&=-(i\mathcal{L}^Q_{\alpha\beta,\alpha'\beta'}+i\mathcal{L}^R_{\alpha\beta,\alpha'\beta'}\delta_{\alpha\alpha'}\delta_{\beta\beta'}\\&\quad+i\mathcal{L}^P_{\alpha\beta,\alpha'\beta'})\hat{\rho}_w^{\alpha'\beta'}(R,P,t),\end{aligned} \tag{8}$$

where

$$i\mathcal{L}^Q\hat{X}_w(R,P)=\frac{i}{\hbar}[\hat{V}_w(R),\hat{X}_w(R,P)]+\frac{\mathbf{P}}{M}\cdot[\hat{\mathbf{D}},\hat{X}_w(R,P)], \tag{9}$$

$$i\mathcal{L}^R\hat{X}_w^{\alpha\beta}(R,P)=\frac{\mathbf{P}}{M}\cdot\nabla_R\hat{X}_w^{\alpha\beta}(R,P), \tag{10}$$

$$i\mathcal{L}^P\hat{X}_w(R,P)=\tfrac{1}{2}(\nabla_P\hat{X}_w(R,P)\cdot\hat{F}+\hat{F}\cdot\nabla_P\hat{X}_w(R,P)), \tag{11}$$

with $\mathbf{F}^{\alpha\beta}(R)=-\langle\alpha|\nabla_R\hat{V}_w(R)|\beta\rangle$. In Eq. (9), $\mathbf{D}^{\alpha\beta}(R)=\langle\alpha|\nabla_R|\beta\rangle$ is the nonadiabatic coupling matrix in the time-independent basis.

B. A wave function approach and the WKB approximation

The mixed quantum-classical Liouville equation is suited specifically for systems where some degrees of freedom need to be treated quantum mechanically while the remaining degrees of freedom obey classical evolution equa-

tions. Generally speaking, one considers light particles with long thermal wavelengths to be more ''quantum'' in nature, while heavy particles exhibit more classical behavior. This is by no means a clear distinction as very often particles play a dual role; a classical particle in one situation can have wavelike properties under other conditions. It is therefore important to examine the criteria which determine the nature of the system. To this end, it is useful to start from a full quantum wave function for the entire system, then select certain degrees of freedom and examine how these degrees of freedom become classical when their corresponding masses becomes relatively large. This may be accomplished by utilizing a WKB expansion to approach the semiclassical limit. In this section we show that a mixed quantum and classical density matrix which satisfies the same quantum Liouville equation as the PWTDM can be obtained from semiclassical arguments.

The full quantum wave function can be written as

$$\Psi=\sum_l \phi_l(r;R)\chi_l(R;t), \tag{12}$$

where $\phi_l(r;R)$ is an orthonormalized local quantum basis which may depend parametrically on the spatial coordinates of the heavy particles R, and $\chi_l(R;t)$ is the heavy particle wave function. In general, the total Hamiltonian can be written in terms of a Hamiltonian $H_q(r)$ for the quantum subsystem, the kinetic energy operator $T_c(R)$ for the heavy particles, and the potential energy term $V_c(r,R)$ which describes the interactions between the heavy particles and the interactions between the light and heavy particles, $H=H_q(r)+T_c(R)+V_c(r,R)$. The choice of the quantum subsystem basis $\phi_l(r)$ is arbitrary. Typically one chooses either a diabatic basis that diagonalizes $H_q(r)$,

$$H_q(r)\phi_l(r)=E_l\phi_r(r), \tag{13}$$

or an adiabatic basis that diagonalizes $H_q(r)+V_c(r,R)$,

$$(H_q(r)+V_c(r,R))\phi_l(r;R)=E_l(R)\phi_l(r;R). \tag{14}$$

In the equations above, r and R stand for vectors of arbitrary dimension and the kinetic energy operator for the classical degrees of freedom is $T_c(R)=-(\hbar^2/2M)\nabla_R^2$. Insertion of Eq. (12) into the Schrödinger equation and projecting onto the l subsystem basis set yields the evolution of the time-dependent wave function for the heavy particles,

$$i\hbar\frac{\partial}{\partial t}\chi_l(R,t)=\frac{1}{2M}(-i\hbar\nabla_R\mathbf{I}-i\hbar\hat{\mathbf{D}})^2_{lk}\chi_k(R,t) + \hat{V}_{lk}\chi_k(R,t), \tag{15}$$

where $\hat{D}_{lk}(R)=\langle\phi_l|\nabla_R|\phi_k\rangle$ and $\hat{V}_{lk}(R)=\langle\phi_l|H_q+V_c|\phi_k\rangle$.

Unlike the usual WKB approximation in which the Schrödinger equation is expanded in powers of $\hbar$, we wish to approach the semiclassical limit by applying the small parameter $\eta=(m/M)^{1/2}\ll 1$, where m and M are the mass of the quantum and classical particles respectively. However it is straightforward to establish by scaling arguments that expanding Eq. (15) in terms of η is equivalent to expansion in powers of $\hbar$.[23] Noting the fact that both the variables R and t in Eq. (15) are on a ''classical'' scale due to the short thermal wavelength of the classical degrees of freedom, we introduce the scaled variables $\eta R'=R$ and $\eta t'=t$. In the scaled variables R' and t', Eq. (15) becomes

$$i\hbar'\frac{\partial}{\partial t'}\chi_l(R',t')=\frac{1}{2M}(-i\hbar'\nabla_{R'}\mathbf{I}-i\hbar'\hat{\mathbf{D}}')^2_{lk}\chi_k(R',t') + \hat{V}_{lk}\chi_k(R',t'), \tag{16}$$

where $\hat{D}'_{lk}=\langle\phi_l|\nabla_{R'}|\phi_k\rangle$ and $\eta\hbar'=\hbar$. Since $\hbar\sim\eta$, it is clear that expanding the Schrödinger equation in powers of $\hbar$ is equivalent to expanding in the small parameter η.

To obtain semiclassical equations for the system, we rewrite the total wave function Ψ as

$$\Psi=\exp\left(\frac{i}{\hbar}\hat{W}(R,t)\right)\sum_l \phi_l(r;R)\chi_l^0(R;t) \tag{17}$$

$$=\sum_{k,l}\phi_k(r;R)T_{kl}(R,t)\chi_l^0(R,t), \tag{18}$$

where $\hat{W}$ is a nonzero, spatially-dependent operator in the quantum subspace which satisfies $\hat{W}^\dagger=\hat{W}$ and

$$T_{kl}(R,t)=\langle\phi_k|\exp(i/\hbar\,\hat{W}(R,t))|\phi_l\rangle. \tag{19}$$

By substituting Eq. (17) into the Schrödinger equation (15) and expansion to order $\hbar^0$ yields the matrix equation

$$\left(\frac{\partial W^{kk'}(R,t)}{\partial t}+\frac{1}{2M}\langle\phi_k|(\nabla_R\hat{W})^2|\phi_{k'}\rangle+V^{kk'}(R)\right) \times T_{k'l}(R,t)\chi_l^0(R,t)=0. \tag{20}$$

Since Eq. (20) holds for arbitrary χ_l^0 and the matrix $T_{k'l}$ is invertible by construction, Eq. (20) implies the operator equation

$$\frac{\partial\hat{W}}{\partial t}+\frac{(\nabla_R\hat{W})^2}{2M}+\hat{V}=0. \tag{21}$$

Next we define the momentum operator $\hat{P}=\nabla_R\hat{W}$, whose time evolution equation can be easily found from Eq. (21),

$$\frac{\partial\hat{P}}{\partial t}=\hat{F}-\frac{1}{2}\left(\frac{\hat{P}\nabla_R\hat{P}}{M}+\frac{\nabla_R\hat{P}\hat{P}}{M}\right), \tag{22}$$

where we have introduced the force operator defined by $\hat{F}=-\nabla_R\hat{V}(R)$. Note that the solution of Eq. (22) is determined when the operator $\hat{P}(R,t')$ is specified at all R for some time t'.

In order to obtain the mixed quantum-classical Liouville equation, we define the row vector $\mathbf{X}(R,t)=(\chi_1(R,t),\chi_2(R,t),\ldots,\chi_L(R,t))$ and the density matrix $\rho_Q(R,t)=\mathbf{X}(R,t)\mathbf{X}^+(R,t)$, where L is the dimension of the quantum subspace and the $\chi_j(R,t)$ are defined in Eq. (12). Utilizing Eq. (17), it is straightforward to obtain the WKB expression for the time evolution of the density matrix $\rho_Q(R,\hat{P}(R,t),t)$,

$$\frac{\partial \rho_Q}{\partial t} = -\frac{1}{M}\nabla_R \cdot (\hat{P}(R,t)\rho_Q)_s - \frac{1}{M}[(\mathbf{D}\cdot\hat{P})_s, \rho_Q] - \frac{i}{\hbar}[\hat{V}, \rho_Q], \quad (23)$$

where $(\hat{A}\hat{B})_s$ denotes the symmetrized product $1/2(\hat{A}\hat{B} + \hat{B}\hat{A})$. Equation (23) describes the evolution of the density matrix at fixed spatial coordinate R and depends on the matrix elements $P^{lm}(R,t)$ of the *time-evolving* operator $\hat{P}(R,t)$. Note that the dependence of the solution ρ_Q on the operator $\hat{P}(R,t)$ implies that it relies on all the matrix elements $P^{lm}(R,t)$, which are obtained from Eq. (22) for a given boundary condition. Furthermore, changing the functional form of the boundary condition for the evolution of $\hat{P}(R,t)$ leads to different evolution of the density matrix ρ_Q. The mixed quantum-classical Liouville equation (7), on the other hand, describes the evolution of the density matrix at fixed scalars R and P. According to the chain rule, the partial derivative of ρ_Q for fixed matrix elements of $\hat{P}(R,t)=\hat{P}$ can be written as

$$\left.\frac{\partial \rho_Q(R,\hat{P}(R,t),t)}{\partial t}\right|_{\hat{P}(R,t)=\hat{P}} = \frac{\partial \rho_Q(R,\hat{P}(R,t),t)}{\partial t} - \left(\frac{\delta \rho_Q}{\delta \hat{P}(R,t)}\frac{\partial \hat{P}(R,t)}{\partial t}\right)_s. \quad (24)$$

Finally, we define the generalized distribution

$$\rho(R,P,t) = Z^{-1}\int \mathcal{D}[\hat{P}](\rho_Q(R,\hat{P}(R,t),t)\,\delta(\hat{P}(R,t)-P\hat{\mathbf{I}}))_s, \quad (25)$$

where the functional integral $\int \mathcal{D}[\hat{P}]$ denotes a functional integral over all matrix elements $P^{lm}(R)$ of the operator $\hat{P}(R,t)$, Z is a normalization factor and $\hat{\mathbf{I}}$ is the unit matrix. It is possible to define other generalized distributions which are consistent with the mixed quantum-classical Liouville equation. Using Eqs. (22)–(25), the evolution of the generalized distribution ρ is

$$\frac{\partial \rho(R,P,t)}{\partial t} = -\frac{i}{\hbar}[\hat{V},\rho] - \frac{P}{M}\cdot\nabla_R\rho - \frac{P}{M}[\mathbf{D},\rho] - \tfrac{1}{2}(\mathbf{F}\cdot\nabla_P\rho + \nabla_P\rho\cdot\mathbf{F}), \quad (26)$$

which is the result of the previous section.

III. THE MULTIPLE THREAD ALGORITHM AND SIMULATIONS ON MODEL SYSTEMS

A. Formulation of the multithreads algorithm

The advantage of solving Eq. (8) instead of the full quantum wave function is that many degrees of freedom are now represented in a classical phase space, and the original multidimensional quantum problem is reduced to solving the simplified coupled evolution equations for the quantum and classical subsystems. The solution of Eq. (8) is by no means trivial, however, since the classical and quantum-mechanical degrees of freedom interact dynamically so that fluctuations in one system affect the other.[19] In order to minimize the interactions between the subsystems, the basis representing the quantum subspace should be carefully chosen such that the classical and the quantum part are separated as much as possible. One good choice of basis to effectively decouple the quantum and classical evolution is the force basis.[21] In what follows, we discuss a numerical scheme based on the mixed quantum-classical Liouville equation for the PWTDM $\hat{\rho}_w$ in the force basis. In this approach, the density matrix is described by an ensemble of matrices following classical trajectories. We will show that through a scheme that requires nothing more than a simple MD propagation and a quantum rotation for each time step, one can achieve asymptotic solutions that agree remarkably well with the exact results for simple model systems.

The fundamental assumption of the multithreads method is that for the time intervals which are of physical interest, $\hat{\rho}_w$ is localized within a finite volume Ω of classical phase space over which its matrix elements represented in a quantum basis are relatively smooth. Under these conditions, a finite number of matrices located at a set of discrete grids points in classical phase space, $\{\hat{\rho}^j(R_j,P_j,t)\}$, $j=1,2,\ldots,L$, can be found which can approximately represent the exact density matrix to any desired accuracy when L is sufficiently large,

$$\hat{\rho}_w(R,P,t) = \sum_{j=1}^{L} \hat{\rho}^j(t)\,\delta(R-R_j(t))\,\delta(P-P_j(t)). \quad (27)$$

For a rank M density matrix, there are $M(M+1)/2$ independent elements which require as many functions to describe their spatial variation. Each function corresponds to a hypersurface in the phase space labeled by the quantum indices, which, in the representation above, is approximated by a set of L discrete grid points. The finite representation of a hypersurface as a set of grid points can be regarded as a hypergrid.

Inserting the finite representation of $\hat{\rho}_w$ in Eq. (27) into the Liouville equation (7) yields[21]

$$\frac{\partial}{\partial t}\rho^j_{\alpha\beta}(t) = i\mathcal{L}^Q_{\alpha\beta,\alpha'\beta'}(R_j,P_j)\rho^j_{\alpha'\beta'}(t), \quad (28)$$

$$\frac{\partial}{\partial t}\delta(R-R_j) = i\mathcal{L}^R(R_j,P_j)\,\delta(R-R_j), \quad (29)$$

$$\rho^j_{\alpha\beta}\frac{\partial}{\partial t}\delta(P-P_j) = i\mathcal{L}^P_{\alpha\beta,\alpha'\beta'}(R_j,P_j)\rho^j_{\alpha'\beta'}\delta(P-P_j), \quad (30)$$

where $i\mathcal{L}^Q$, $i\mathcal{L}^R$, and $i\mathcal{L}^P$ are the Liouville operators for the quantum and the classical phase space defined in Eqs. (9)–(11). In the basis that diagonalizes the force operator $\hat{F}$, Eq. (30) can be rewritten as

$$\left(\frac{\partial}{\partial t}\right)_{\alpha\beta}\delta(P-P_j) = -\frac{1}{2}[\mathbf{f}_\alpha(R_j)+\mathbf{f}_\beta(R_j)]\cdot\frac{\partial}{\partial P}\delta(P-P_j), \quad (31)$$

where $\mathbf{f}_\alpha$ is the force eigenvalue, $\hat{F}_w|\alpha\rangle = \mathbf{f}_\alpha|\alpha\rangle$. In the absence of the quantum rotation, different hypersurfaces decouple, which implies that grids for different quantum indices α,β of the PWTDM evolve independently and the value of density matrix element remains constant while the grid coordinate propagates along a classical trajectory. However, the presence of quantum rotations introduces coupling between the surfaces and leads to nontrivial evolution of the matrices ρ^j.

In order to examine how grid weights evolve, it is instructive to look at the formal solution of Eq. (28) for a single time step,

$$\tilde{\rho}(R_i,P_i,t+\Delta t) = e^{i\tilde{\mathcal{L}}^Q(R_i,P_i)\Delta t}\tilde{\rho}(R_i,P_i,t), \tag{32}$$

where $\tilde{\rho}(R_i,P_i)$ denotes the density matrix arranged in a supervector form and $i\tilde{\mathcal{L}}^Q$ is a supermatrix representing the quantum Liouville operator. The supermatrix $i\tilde{\mathcal{L}}^Q$ is determined by the nonadiabatic coupling matrix $\mathbf{D}$, and approaches the unit operator as $\mathbf{D}\rightarrow 0$. The operand on the right-hand side of Eq. (32) is the supervector for a particular hypersurface and contains only one nonzero matrix element of vector index i. As a result of the quantum operation, the final state on the left-hand side will generally have as many nonzero elements as its dimension. These include a nonzero value with the same vector index i as the nonzero element of the initial state, as well as nonzero values at (possibly) all other indices $j\neq i$. Note that the matrix elements corresponding to indices $j\neq i$ are higher order in Δt. It is convenient to call the original nonzero index i the primary term, and the other indices j secondary terms. As grid points are grouped by matrix indices, the secondary terms are new grid points that belong to other hypersurfaces. Thus the effect of the quantum rotation is to generate new grid points, or threads on all the hypergrids. If initially all hypergrids representing the density matrix elements contain equally l grid points, then after one quantum rotation the total number of grid points or threads will increase by a factor of $M(M+1)/2$ as each hypergrid will contain $M(M+1)/2\times l$ grid points after regrouping. Thus it is clear that the total number of threads grows by a factor of $M(M+1)/2$ each time a quantum rotation occurs, which very rapidly becomes overwhelmingly large. On the other hand, since the function the weighted grid points represent is localized and sufficiently smooth by assumption, it can be approximated to arbitrary accuracy by a finite number of grids. Therefore, from a practical point of view, many new grids generated by the quantum rotation are redundant. This suggests a procedure[21] in which the less relevant grids (threads) are absorbed by (combined with) the more relevant ones. Thus the new grid generation, or thread ''branching,'' is counterbalanced by rules to reduce the total number of threads to a manageable level.

Obviously the key to formulating an effective algorithm is the manipulation of the threads to best describe the evolving hypersurfaces while maintaining a finite number of total threads. The most obvious thread reduction rule is to combine threads which are nearby in classical phase space. If the elements of the density matrix are sufficiently smooth functions in a particular region on the hypersurfaces, only a few grid points are necessary in that region to approximate the function with reasonable accuracy. Therefore if two threads approach one another in the smooth region on a hypersurface, one is likely to be redundant and can be dropped from the hypergrid or absorbed by the other thread. The simplest way to implement a thread reduction procedure is to find and order all nearest thread pairs and then to combine as many threads as necessary to maintain a constant number of total threads. As the propagation time between branching events and the total number of threads determine the threshold distance for combining threads, the time step can be dynamically adjusted to maintain energy conservation for a given number of threads. Alternatively, the total number of threads can be varied for a given time step until energy conservation and convergence of observables is observed. In terms of computational expense, the procedure has two components which scale differently with the total number of threads. One part consists of the potentially costly task of constructing the adiabatic matrix elements and coupling terms, which scales linearly with the number of threads. The other part consists of a searching algorithm to identify adjacent threads. Typically, such algorithms scale as the square of the total number of threads for small numbers of threads, although sophisticated routines may reduce the computational cost to some extent. These simple rules have been tested and shown to work remarkably well, even in strongly nonadiabatic systems or systems with low kinetic energy where tunneling is important.[21]

As an alternative to these rules, one can use considerations of the conservation laws to construct other thread combination rules to improve the accuracy or efficiency of the method. For example, instead of letting one thread absorb another, a new thread can be generated as a result of combining the two adjacent threads, with the new thread placed to best maintain the conservation laws. To illustrate how thread combination rules can be based on conservation principles, suppose we have two nearby threads $\rho_1^{\alpha\beta}$ and $\rho_2^{\alpha\beta}$ at classical phase space positions (R_1,P_1) and (R_2,P_2), respectively. Local population conservation requires that $\mathrm{Tr}\,\hat{\rho}' = \mathrm{Tr}\,\hat{\rho}_1 + \mathrm{Tr}\,\hat{\rho}_2$, where $\hat{\rho}'$ is the density matrix associated with the new thread, which suggests the superposition rule, $\hat{\rho}' = \hat{\rho}_1 + \hat{\rho}_2$. Note that as the off-diagonal elements of the density matrix are complex numbers, the superposition rule specifies that the imaginary part of the density matrix for the combined thread is obtained by adding the imaginary parts of the combining threads. It is possible that other phase combination rules which are consistent with the linearity of the quantum Liouville equation are equally useful. In addition to the combination of the matrices at nearby grid points, a rule to specify the placement of the thread in phase space must be adopted. For the case of the threads representing the diagonal elements of the density matrix $\rho^{\alpha\alpha}\delta_{\alpha\beta}$, we propose that the placement of the thread should be determined by the equation $\mathrm{Tr}(x\hat{\rho}') = \mathrm{Tr}(x_1\hat{\rho}_1) + \mathrm{Tr}(x_2\hat{\rho}_2)$, where x is the phase space coordinate. For the case when $\alpha\neq\beta$, however, a suitable thread combination rule is less obvious. For the numerical studies presented in the next section, the weighted phase point average $x = (|\rho_1^{\alpha\beta}|x_1 + |\rho_2^{\alpha\beta}|x_2)/(|\rho_1^{\alpha\beta}| + |\rho_2^{\alpha\beta}|)$

has been used, although other prescriptions for combining threads on hypersurfaces corresponding to off-diagonal matrix elements of $\hat{\rho}_w$ are likely to work as well.

B. Results on model systems

We have tested the simple thread combination rules elaborated in the previous section on model two level systems recently studied by other authors.[2,3,7,24] These models have been devised specifically to test particular quantum scattering features which mixed quantum-classical simulations must reproduce.[3] In all the tests, the results of the multithreads algorithm are compared to exact (converged) quantum calculations of the models which were carried out using fast Fourier transform (FFT) methods on a grid of 4096 points. For the quantum calculations, the initial wave function was a Gaussian wave packet of momentum $\hbar k$ centered at R_0,

$$\psi(R)=(\pi\sigma^2)^{-1/4}\exp(-(R-R_0)^2/2\sigma^2)\times\exp(ik(R-R_0)), \tag{33}$$

where $\sigma=2.5176$ a.u. and $M=2000$ was the nuclear mass of the particle. The multithreads calculations were carried out by propagating the initial partially-transformed Wigner density matrix represented by a finite number of threads [see Eq. (27)]. In general, no more than several hundred threads were used to represent the density matrix. The propagation time step for both the quantum and multithreads calculation was set to be on the order of 1 a.u. to ensure energy conservation.

1. Dual avoided crossing model

The dual avoided crossing model is composed of two diabatic surfaces intersecting twice,[3] with the couplings leading to quantum interference which produces oscillations in transition probability as a function of initial energy. The complicated quantum interference pattern makes the model a rigorous test for quantum-classical dynamics, particularly in the low energy regime where tunneling is important. The diabatic potentials and coupling, expressed in atomic units, are

$$V_1=0, \tag{34}$$

$$V_2=-0.1\exp(-0.28R^2)+0.05, \tag{35}$$

$$V_{12}=0.015\exp(-0.06R^2). \tag{36}$$

In the quantum dynamics simulation of this model, an adiabatic ground-state wave packet starting in the asymptotic region $R_0=-8$ a.u. propagates toward the region of coupling of the diabatic surfaces whereupon it is partially transmitted through the coupling region with populations in the ground and excited state and partially reflected back, again with populations in the ground and excited state. The detailed dynamics of the system can be probed by calculating the probability of transmission and reflection in the ground and excited states. In Fig. 1 the results of the exact quantum and multithreads calculation for the probability of transmission in the ground state are plotted as a function of the logarithm of the initial energy. For the parameters specified for this model, however, the exact quantum calculation reveals negligible reflection. The multithreads results were obtained using 300 threads propagating from the initial phase point $(R_0,\hbar k)$. For the runs at low energy it was necessary to reduce the time steps by a factor of 5 in the region of strong nonadiabatic coupling to maintain energy conservation. Each multithread calculation took a few minutes on a DEC Alpha 21164 workstation. As is evident from Fig. 1, the agreement of the multithreads calculation with the quantum calculation is within 1% over the *entire* energy range, including the low energy regime where tunneling is prominent. As can be seen in Fig. 1, the multithreads calculation is also capable of reproducing all the Stueckelberg oscillations that result from the quantum interference due to the nonadiabatic couplings, including the oscillation at low energy. In contrast, the MDET method of Tully and co-workers[3] and the mean-field with surface hopping method (MFSH) of Prezhdo and Rossky[2] show more significant deviation from the exact results, particularly at low energies. The deviations in their results from the exact results are likely due to the surface-hopping rule, which relies on classical energy conservation rules which are violated at low energies. Similarly, the multiple-spawning method of Martínez and co-workers[24] show deviations on the order of 10% in the low energy region. In order to demonstrate the rapid convergence of the multithreads method, in Fig. 2 the ground state population as a function of the time-evolving expectation value of the spatial coordinate is plotted along with the exact FFT solution of the mixed quantum-classical Liouville equation for a very narrow initial distribution initially centered at $R=-8.0$ a.u. and $\hbar k=17$ a.u. From Figs. 2 and 3, in which the average trajectory is plotted for a number of different maximum thread values, it is evident the method converges quickly for this model, giving converged results for as few as 300 threads.

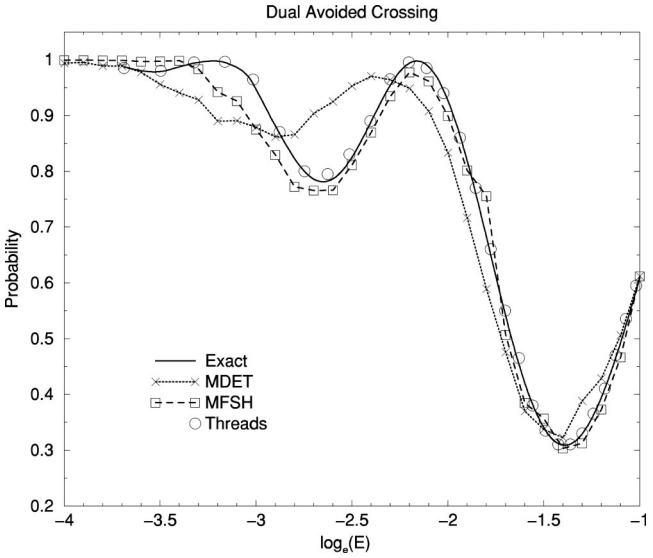

FIG. 1. Transmission probability of the lower quantum state for the dual-crossing model. Solid lines, crosses and dotted line, squares and dashed line, and *unconnected* circles indicate the exact quantum, MDET, MFSH, and multithreads data, respectively.

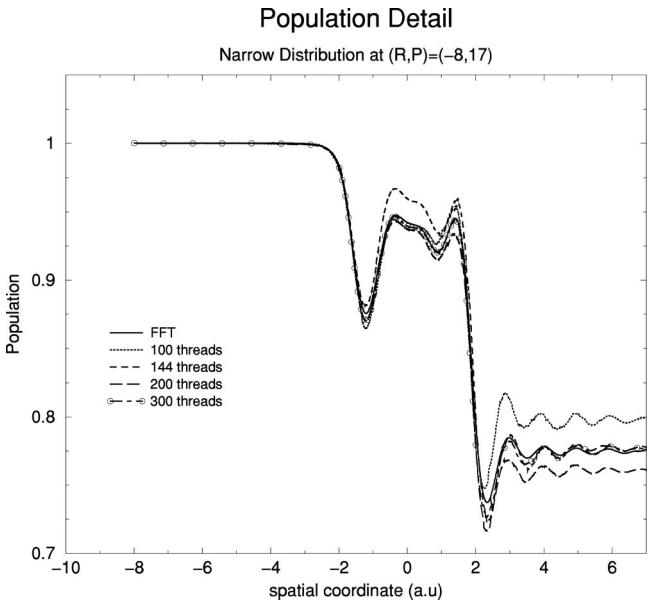

FIG. 2. Lower state population as a function of the wave packet center for different number of threads. The solid line is the exact FFT solution of the mixed quantum-classical Liouville equation.

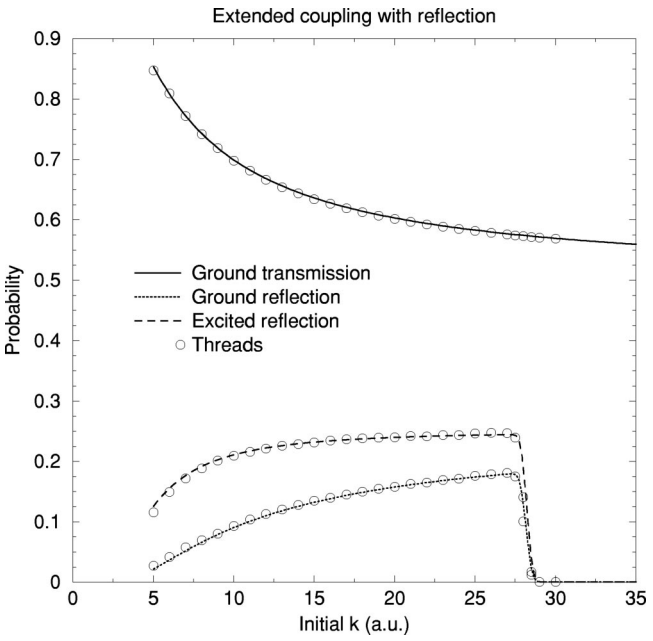

FIG. 4. Exact probabilities of ground state transmission (solid), ground state reflection (dotted), and reflection of the excited state (dashed). Unconnected circles are corresponding results from the multithreads method.

2. Extended coupling with reflection model

The second model system considered here is comprised of two nearly degenerate energy surfaces coupled by a strong interaction with significant spatial extent.[2,3] The diabatic potentials and coupling for the system in atomic units are $V_1 = -V_2 = -0.0006$ and

$$V_{12} = \begin{cases} 0.1\exp(0.9R) & \text{if } R<0 \\ 0.1[2-\exp(-0.9R)] & \text{otherwise.} \end{cases} \tag{37}$$

The model is designed to simulate the case in which an initially localized wave packet splits into two parts upon entering the coupling region, where the part of the wave function on the excited adiabatic surface is reflected while the wave function on the ground state is transmitted. In Fig. 4, the results of the exact quantum calculation of the ground state transmission probability, ground state reflection probability and excited state reflection probability are plotted as a function of the initial momentum of the wave packet along with results from the multithreads calculation (*unconnected* circles). For the quantum dynamics calculation, the initial wave packet was centered in the asymptotic region with $R_0 = -12.0$ a.u., while the multithreads calculation was performed by averaging over 100 realizations of the multithread evolution, with each realization starting from a classical phase point (R_0, P_0) drawn independently from the initial semiclassical distribution $\hat{\rho}_w$. Each realization of the evolution showed convergent results for a maximum thread number of 100. As is evident from Fig. 4, the multithreads results agree perfectly with the exact results within statistical uncertainties associated with drawing from the initial distribution. The uncertainties arise due to the influence of the width of the semiclassical distribution in momentum, which is particularly significant in the region near $k=28$ a.u., where the reflection probabilities drop rapidly to zero. Note that in contrast to other mixed quantum-classical molecular dynamics methods, there is no evidence of artificial oscillations in the reflection probabilities.

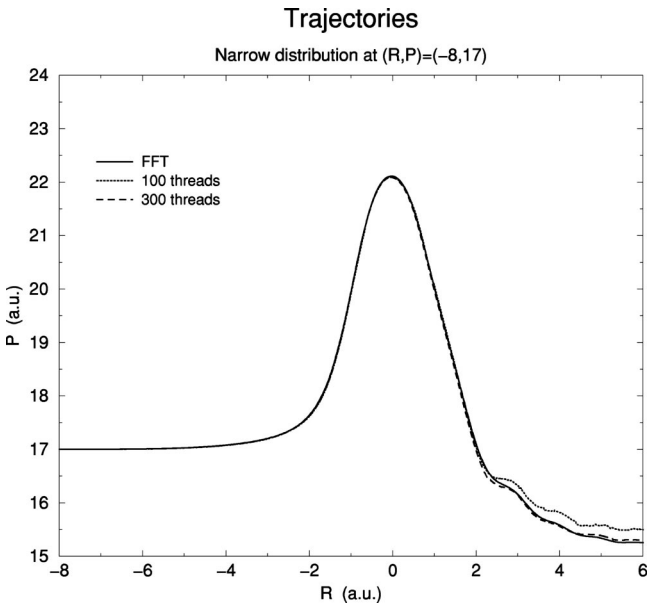

FIG. 3. Phase space trajectory for different number of threads. The solid line is the exact FFT solution of the mixed quantum-classical Liouville equation.

IV. DISCUSSION AND CONCLUSIONS

The multithreads algorithm has performed remarkably well on model systems at relatively little computational cost. The numerical simplicity and efficiency of the method can be attributed to the local nature of the procedure, where all quantities required at each time step are computed locally spatially and temporally. In methods incorporating similar ideas, such as the FMS algorithm of Martínez and

co-workers,[12] time-consuming calculations of overlap matrices of evolving basis functions must be calculated which detract from their efficiency. In the current method, the use of the force representation decouples the density matrix evolution from the evolution of the grid points, and the interaction between matrix elements appears in the form of thread branching and recombination. In this sense, the threads interact with one another dynamically as the system evolves. In contrast, Martens and co-workers[9] propose a method of solution of the mixed quantum-classical Liouville equation in which an ensemble of classical trajectories is evolved in the adiabatic basis according to classical equations corresponding to a Hamiltonian for that matrix element. Each trajectory in the ensemble for a particular matrix element is independent of all others and depends only on the initial phase space point. To describe the evolution of the density matrix, the weight of the each of the trajectories in the ensemble is calculated at each time step through an interpolation scheme.

Although one is generally interested in expectation values and moments of the density matrix, the time-dependent weights of each of the trajectories for the density matrix elements can be used to reconstruct the phase-space structure of the elements of the density matrix for low dimensional systems by broadening the delta-function distributions to narrow Gaussians of finite width in the representation of the density matrix. This approach has been demonstrated to give excellent agreement with exact distribution functions for a one-dimensional nonadiabatic model[13] using a similar propagation scheme.

For all numerical schemes the moment of truth comes when they are applied to a real problem, such as the dynamics of a chemical reaction involving a large number of classical degrees of freedom. Such studies are currently underway. However we anticipate that the present algorithm will scale nicely with dimension due to the fact that for short time intervals, the propagation of the momenta governed by the operator $i\mathcal{L}^P$ [see Eq. (11)] can be decomposed through a Trotter expansion into the equations of motion for each classical degree of freedom. For example, suppose R represents the multidimensional spatial vector $R=(r_1,r_2,\ldots,r_N)$, and $\hat{F}^i$ is the force matrix associated with r_i. If the force matrices $\{\hat{F}^i\}$ do not commute with one another, then the momenta for all noncommuting degrees of freedom must be updated in consecutive steps, each one along one classical r_i and P_i direction. In addition, the density matrix must be transformed into the appropriate force representation before each step. Since each propagation in P_i direction involves one branching transformation, there will be a total N branching events for N dimensions. For an intrinsically quasi-one-dimensional system in which the spread in phase space is localized along a few degrees of freedom determined by the directional off-diagonal coupling matrix **D**, the thread combination rules will guarantee that the threads will remain concentrated along a few main paths. Furthermore, although the transformations to different force representations must be done frequently, each transformation requires little computational work since the quantum subspace is small for problems involving only a few adiabatic energy surfaces.

The multithreads algorithm for systems of high dimensionality is much simpler when the force matrices $\hat{F}^i$ commute. For many systems of physical interest, the majority of classical degrees of freedom are either uncoupled or weakly coupled to the quantum subsystem. For these degrees of freedom, the force matrices $\hat{F}^i$ either commute or have no quantum character. If all the force matrices commute, a single transformation can diagonalize all the force matrices and the propagation in the phase space can be done in a single step. An interesting possibility is a system where the quantum subspace is reducible, and each reduced subspace couples to certain classical degrees of freedom. To date, only the most simple thread combination rules have been used in our simulations. For a more complicated multidimensional problem, it is likely that more sophisticated thread combination rules will lead to improved performance of the algorithm.

ACKNOWLEDGMENTS

This work was supported by a grant from the Natural Sciences and Engineering Research Council of Canada. The authors would like to thank D. F. Coker for his quantum dynamics code and P. J. Rossky for providing the MFSH data for the model systems. The authors would also like to thank R. Van Zon for useful discussions.

[1] V. S. Filinov, S. Bonella, Y. L. Lozovik, A. V. Filinov, and I. Zacharov, in *Classical and Quantum Dynamics in Condensed Phase Simulations*, edited by B. J. Berne, G. Ciccotti, and D. Coker (World Scientific, Singapore, 1998).
[2] O. V. Prezhdo and P. J. Rossky, J. Chem. Phys. **107**, 825 (1997).
[3] J. C. Tully, J. Chem. Phys. **93**, 1061 (1990).
[4] J. C. Tully, Int. J. Quantum Chem. **25**, 299 (1991); S. Hammes-Schiffer and J. C. Tully, J. Chem. Phys. **101**, 4657 (1994).
[5] J. L. McWhirter, J. Chem. Phys. **108**, 5683 (1998).
[6] F. Webster, P. J. Rossky, and R. A. Friesner, Comput. Phys. Commun. **63**, 494 (1991); F. J. Webster, J. Schnitker, M. S. Friedrichs, R. A. Friesner, and P. J. Rossky, Phys. Rev. Lett. **66**, 3172 (1991).
[7] D. F. Coker and L. Xiao, J. Chem. Phys. **102**, 496 (1995).
[8] X. Sun and W. H. Miller, J. Chem. Phys. **106**, 916 (1997); **106**, 6346 (1997).
[9] C. C. Martens and J.-Y. Fang, J. Chem. Phys. **106**, 4918 (1997); A. Donoso and C. C. Martens, *ibid.* **112**, 3980 (2000).
[10] Raymond Kapral and Giovanni Ciccotti, J. Chem. Phys. **110**, 8919 (1999).
[11] G. Stock and M. Thoss, Phys. Rev. Lett. **78**, 578 (1997).
[12] M. Ben-Nun and T. J. Martínez, J. Chem. Phys. **108**, 7244 (1998); T. J. Martínez and R. D. Levine, J. Chem. Soc., Faraday Trans. **93**, 940 (1997); T. J. Martínez, M. Ben-Nun and R. D. Levine, J. Phys. Chem. **101**, 6389 (1997).
[13] A. Donoso, D. Kohen, and C. C. Martens, J. Chem. Phys. **112**, 7345 (2000).
[14] For a review of quasiclassical trajectory methods, see *Advances in Classical Trajectory Methods*, edited by W. L. Hase (Jai, London, 1992), Vol. 1.
[15] W. H. Miller, J. Chem. Phys. **95**, 9428 (1991); E. J. Heller, *ibid.* **94**, 2723 (1991); **95**, 9431 (1991); G. Stock and M. Thoss, Phys. Rev. Lett. **78**, 578 (1997); M. F. Herman and E. Kluk, Chem. Phys. **91**, 27 (1984); K. G. Kay, J. Chem. Phys. **100**, 4377 (1994); **100**, 4432 (1994).
[16] X. Sun, H. Wang, and W. H. Miller, J. Chem. Phys. **109**, 7064 (1998).
[17] P. Pechukas, Phys. Rev. **181**, 166 (1969).
[18] J. C. Tully and R. K. Preston, J. Chem. Phys. **55**, 562 (1971).
[19] W. Boucher and J. Traschen, Phys. Rev. D **37**, 3522 (1988).
[20] O. V. Prezhdo and V. V. Kisil, Phys. Rev. A **56**, 162 (1997).
[21] C. C. Wan and J. Schofield, J. Chem. Phys. **112**, 4447 (2000).
[22] A. Anderson, Phys. Rev. Lett. **74**, 621 (1995).
[23] G. A. Hagedorn, Commun. Math. Phys. **77**, 1 (1980).
[24] T. J. Martínez, M. Ben-Nun, and R. D. Levine, J. Phys. Chem. **100**, 7884 (1996).